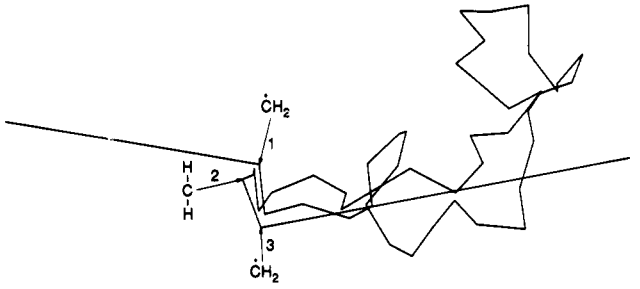

Figure 7. A close-up of the coiled region between atoms 2 and 3 in Figure 4.

depicted in eq 6 which involves the transfer of a hydrogen from atom 2 to atom 1 and the formation of a double bond between atoms 2 and 3.

Summary and Conclusions

A model based on molecular dynamics was used to investigate the kinetic stability of polymers as a function of temperature, secondary structure, and molecular weight. Temperatures and atomic velocity distributions, as well as the progress of random scission reactions, were monitored as a function of time and were found to be consistent with statistical predictions for these properties. In particular, we observed that the atomic velocities reorganized into Maxwell-Boltzmann distributions almost instantaneously and that the average heat capacities of the model polymers were equal to 2.3 and 2.6 Nk_B for the coiled and planar zigzag models, respectively.

Computer-generated rates of random scission for both planar zigzag and coiled model polymers were found to correlate reasonably well with the functional predictions of RRK theory. The rate constants for random scission of the planar zigzag model polymers, however, were about 4 times as large as the corresponding values for coiled polymers with the same primary structure. The computer simulations indicated further that the thermal stability of individual model polymers increased with decreasing molecular weight but that the rate of degradation per unit mass of sample was independent of the molecular weight distribution of the polymer.

Still frames from computer movies of the thermal motions of model polymers have revealed pronounced coilings in the vicinity of dissociating bonds which are consistent with proposed mechanisms for hydrogen transfer. Of particular interest is the observation that the coiling which accompanies bond dissociations in extended chains tends to stabilize the polymer, making further scissions increasingly more difficult. This interplay constitutes a mechanism for self-regulation that may influence mass-loss rates and product distributions in degrading polymers.

Acknowledgment. M.N. thanks Dr. Howland Fowler of the Center for Computing and Applied Mathematics (NIST) for providing technical assistance in making the computer movies and Dr. Edmund DiMarzio of the Polymers Division (NIST) for many helpful discussions.

Sol-Gel Polymerization Studied through ^{29}Si NMR with Polarization Transfer

F. Brunet,*,†,‡ B. Cabane,†,‡ M. Dubois,‡ and B. Perly‡

Commissariat à l'Energie Atomique, Centre d'Etudes Nucleâires de Saclay, F-91191 Gif-sur-Yvette Cedex, France *(Received: January 23, 1990; In Final Form: July 9, 1990)*

Silicon tetramethoxide (TMOS) monomers have been dissolved in mixtures of methanol and water, hydrolyzed, and condensed to form siloxane polymers. The various oligomers which form during the early stages of the reaction have been identified through high-resolution ^{29}Si NMR with polarization transfer. At low water/alkoxide ratios the hydrolysis is incomplete and limits the condensation reaction. Small cyclics are formed in addition to linear polymers. At high water/alkoxide ratios, the hydrolysis is fast and complete and the condensation is rate limiting. The polymers are largely branched as indicated by the high proportion of Q^3 chain branching sites and Q^4 three dimensionally cross-linked groups. So highly condensed species including small rings or cagelike structures can be expected in these mixtures.

Introduction

Sol-gel technology is a promising route for the obtaining ceramics, glasses, and fibers of high purity and homogeneity.[1] This process involves the hydrolysis and condensation of metal alkoxides $\{M(OR)_n\}_m$ in organic or aqueous solvents.[1,2] Extensive condensation produces cross-linked polymers which entrap the solvent in a macroscopic gel. The gel can be used in its "wet" form (alcogel), or it can be dried to yield a porous material (xerogel, aerogel), and then it can be sintered to a dense glass or ceramic.

In the hydrolysis step (eq 1), the alkoxides groups are replaced stepwise by hydroxide groups:

$$Si(OR)_4 + nH_2O \rightarrow Si(OR)_{4-n}(OH)_n + nROH \quad (1)$$

In the condensation step (2), reactions occur between partially (2a) or totally (2b) hydrolyzed species:

$$Si\text{–}OR + HO\text{–}Si \rightarrow \text{–}Si\text{–}O\text{–}Si\text{–} + ROH \quad (2a)$$

$$Si\text{–}OH + HO\text{–}Si \rightarrow \text{–}Si\text{–}O\text{–}Si\text{–} + HOH \quad (2b)$$

The overall balance is

$$Si(OR)_4 + 2H_2O \rightarrow SiO_2 + 4ROH \quad (3)$$

2 mol of H_2O being required to form 1 mol of silica gel.

However, the reactions are incomplete, and the product is not dense silica. Instead, they produce polymers with a siloxane backbone and SiOH or SiOR side groups. There are many ways in which such polymers can be linked, and this structure determines the properties of the material, e.g., its surface area, its viscosity (before the gel point) and its mechanical properties (after the gel point). Recent investigations[3] have shown that the early steps of the polymerization are very important for the course of the reaction, since they determine the subunits from which the polymers are made. These early steps can be studied through NMR spectroscopy.[3-6] In particular, valuable information

†CNRS URA 331.
‡CEA DSM/DPhG/SCM.

(1) Brinker, C. J.; Clark, D. E.; Ulrich, D. R. *Mater. Res. Soc. Symp.* **1984**, 32.
(2) Iler, R. K. *The Chemistry of Silica*; Wiley: New York, 1979.
(3) Pouxviel, J. C.; Boilot, J. P.; Beloeil, J. C.; Lallemand, C. *J. Non-Cryst. Solids* **1987**, 89.
(4) Kelts, L. W.; Effinder, N. J.; Mepolder, S. M. *J. Cryst. Solids* **1986**, *83*, 353.

0022-3654/91/2095-0945$02.50/0

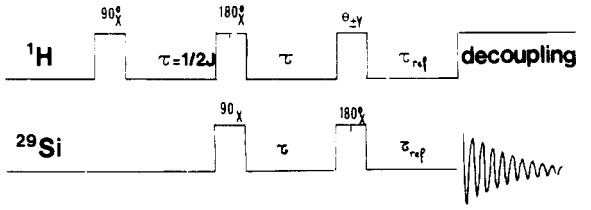

Figure 1. Pulse scheme for DEPT: τ is the transfer time ($=1/2J$) and θ the variable pulse angle (multiplet selection); τ_{ref} is the refocusing time.

concerning the substitution of side groups and the organization of Si–O–Si links can be obtained from the chemical shifts of ^{29}Si nuclei.[7-9]

The main difficulty with this problem is the very large number of substitutions that are possible for a given backbone, and also the large number of isomers that are possible even with a small number of silicon atoms. One advantage of ^{29}Si NMR is that many of these configurations are resolved into separate lines.[3,6] However, it has proven difficult to assign all of these lines unambiguously, even for the early stages of the polymerization process because chemical shifts vary with medium effects (pH, T, degree of hydrolysis).

Here we show that such problems can be overcome through the use of ^{1}H–^{29}Si polarization transfer.[10] This technique allows ^{29}Si to be identified according to the number of protons that are coupled to them. In addition the polarization transfer brings a large increase in the signal of ^{29}Si nuclei. We apply this method to investigate the polymerization of silicon tetramethoxide (TMOS) and we show how this polymerization depends on the degree of hydrolysis and on the pH of the solvent.

Materials

In these experiments silicon tetramethoxide is the starting monomer, water is used to hydrolyze it, and methanol is the common solvent. A critical parameter is the molar ratio $w = H_2O/TMOS$; this determines the possible extent of hydrolysis, with stoichiometry at $w = 4$. We used $w = 2.8$ (incomplete hydrolysis) and $w = 8$ (twice the amount needed for full hydrolysis). The other main parameter is pH; hydrolysis is catalyzed by H^+ ions, and it becomes quite efficient at pH values below pH = 3. Condensation depends on acid–base equilibria of the silanols, and it is efficient when they are ionized either as SiO^- (pH > 3) or as $SiOH_2^+$ (pH < 2). We used pH values of 1.5 and 3 where hydrolysis is fast and condensation slow; in this way the time scales of both reactions are largely decoupled. The last parameter is the concentration of monomers; we used equal volumes of TMOS and methanol, and hence the volume fraction of SiO_2 in the resulting gels is 8% ($w = 2.8$) or 6% ($w = 8$); this is a concentrated regime.

Polarization-Transfer Method

The low sensitivity of ^{29}Si (natural abundance 4.7% and small negative γ) severely limits NMR measurements. In addition the efficiency of recording decoupled spectra is further reduced by the negative nuclear Overhauser effect NOE due to the dipolar coupling of negative γ_s of ^{29}Si nucleus and γ_H, and also by the slow relaxation of ^{29}Si nucleus. But the recent development of multipulse NMR techniques,[11-13] all based on the transfer of the large proton polarization to nuclei with low γ through the scalar spin–spin coupling, leads to great sensitivity enhancements compared with normal FT NMR spectroscopy. In the present work we used the DEPT sequence (distortionless enhancement by polarization transfer) which is shown Figure 1. The advantage in the DEPT experiments is that the normal multiplet structures are retained in the polarization transfer spectra. The theoretical signal enhancement E_d of ^{29}Si decoupled spectra depends upon three variables: τ (transfer time), θ (variable pulse angle), and n, the number of protons coupled to ^{29}Si:[12]

$$E_d = n(\gamma(^1H)/\gamma(^{29}Si)) \sin\theta \cos^{n-1}\theta \sin(\pi J\tau) \qquad (I)$$

In this equation only the methyl protons are counted because the OH groups exchange rapidly and cannot contribute to the signal enhancement. The only two parameters that may be adjusted to optimize the enhancements are the transfer time τ and the variable pulse angle θ. Optimal enhancement is achieved when τ is set to $1/(2J)$ (where J is the ^{1}H–^{29}Si coupling constant) and θ to the following value:

$$\theta_{opt} = \arcsin^{-1}(1/n^{1/2}) \qquad (II)$$

Figure 2 shows the theoretical variation of intensities with pulse angle θ, calculated according to eq I with τ equal to $1/2J$. This variation provides a tool for distinguishing the number n of protons attached to ^{29}Si. For large θ values ($\theta > 90°$) the distinction between SiH_n groups where n is odd or even is obvious. Another advantage of this technique is that the limiting repetition rate now depends upon the relaxation time of attached protons which is always shorter than that of Si, allowing faster data acquisition. Nevertheless the performance of the DEPT sequence depends critically upon correct calibration of the 90° pulses ^{29}Si and ^{1}H. It also depends upon transfer time τ and spin–spin relaxation time T_2 ratio. For small J values ($J < 10$ Hz), the transfer time increases ($\tau = 1/2J$) and the DEPT sequence length may approach T_2, leading to severe intensity losses through relaxation. In our experiments the transfer time τ was optimized to 142 ms taking into account the measured ^3J(Si–H) scalar coupling value (3.5 Hz) for $Si(OCH_3)_4$. At medium H_2O concentration ($w = 2.8$) the DEPT sequence was used with a mean value of θ equal to 24° to make the signals SiH_n (n = 3, 6, 9, 12) observable with good intensity (I(6H) = 100%, I(9H) = 94%, I(3H) = 89%, I(12) = 87%). Quantitative results may be obtained from a single experiment after the integrated intensities are corrected.

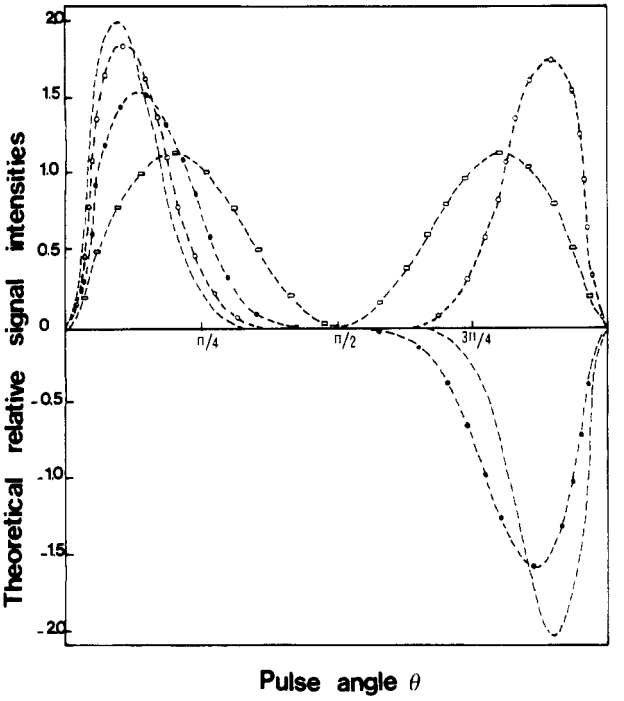

Figure 2. Theoretical relative signal intensities with variable θ pulse angle using DEPT for SiH_n groups (n is the number of protons coupled to ^{29}Si): 12H, ---, θ_{opt} = 17°; 9H, -○-, θ_{opt} = 19°; 6H, -●-, θ_{opt} = 24°; 3H, -□-, θ_{opt} = 36°.

(5) Artaki, I.; Zerda, T. W.; Jonas, J. *Mater. Lett.* **1955**, *3*, 493.
(6) Artaki, I.; Bradley, M.; Zerda, T. W.; Jonas, J. *J. Phys. Chem.* **1985**, *89*, 4399.
(7) Harris, R. K.; Knight, C. T. G. *J. Chem. Soc., Faraday Trans. 2* **1983**, *79*, 1525.
(8) Harris, R. K.; Knight, C. T. G. *J. Chem. Soc., Faraday Trans. 2* **1983**, *79*, 1539.
(9) Engelhardt, G.; Altenburg, W. *Z. Anorg. Allg. Chem.* **1977**, *43*, 428.
(10) Blinka, T. A.; Helmer, B. J.; West, R. *Adv. Organomet. Chem.* **1984**, *23*, 193.
(11) Doddrell, D. M.; Pegg, D. T.; Bendall, M. R. *J. Magn. Reson.* **1982**, *48*, 323.
(12) Bendall, M. R.; Pegg, D. T. *J. Magn. Reson.* **1983**, *53*, 272.
(13) Burum, D. P.; Ernst, R. P. *J. Magn. Reson.* **1980**, *39*, 163.

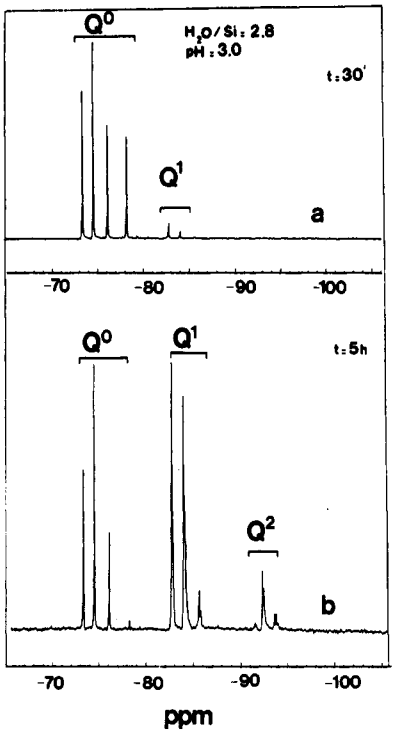

Figure 3. ^{29}Si NMR spectra of the $TMOS/CH_3OH/H_2O$ mixture in 1/3.7/2.8 molar ratio obtained at 295 K by using DEPT sequence (transfer time 142 ms; relaxation delay 10 s; number of transients 16): (a) after 30 min; (b) after 5 h.

Assignment of ^{29}Si Lines

The ^{29}Si chemical shifts range extends from −70 to about −120 ppm and in this range four groups of lines show up with different shifts.[7,8] These groups are usually named Q^n, where Q represents a silicon atom and n is the number of siloxane bonds attached to silicon. So Q^0 represents monomeric groups, Q^1 end groups of chains, Q^2 middle groups in chains or cycles, Q^3 chain branching sites, and Q^4 fully cross-linked groups. In this section we present assignments of individual resonances for groups Q^0, Q^1, and Q^2 through the DEPT pulse angle analysis.

A. Incomplete Hydrolysis. Figure 3 shows ^{29}Si NMR spectra obtained at very early stages of the polymerization in the mixture $TMOS/CH_3OH/H_2O$ with molar ratio 1/3.7/2.8. After 5 h no Q^3 or Q^4 species are visible and only species up to Q^2 are observed (Figure 3b). The ^{29}Si resonance lines are very sharp ($\Delta\nu$ = 0.8–1 Hz). The dependence of signal intensities with the θ pulse length is in good agreement with the theoretical values respectively expected for Si $(OCH_3)_{4-n}(OH)_n$ groups with n = 1, 2, and 3 (Figure 4a). So the different hydrolyzed species corresponding respectively to structural units $Q^0(1,3)$, $Q^0(2,2)$, and $Q^0(3,1)$ can be easily identified according to their chemical shifts. By use of the same method the Q^1 condensed species have been identified and resolved into different structural units $Q^1(0,3)$, $Q^1(1,2)$, and $Q^1(2,1)$ characterized by their chemical shifts (Figure 4b). The totally hydrolyzed species $Q^0(4,0)$ and $Q^1(3,0)$ cannot be observed by polarization transfer but are expected to resonate at lower field (Table I). Our attributions for Q^0 and Q^1 structural units are in good agreement with literature data.[4,6-9]

For Q^2 condensed species weak resonances at −91.40 and −93.70 ppm are observed with a more intense signal at −92.40 ppm. By use of polarization-transfer methods the peak at −93.70 ppm has been assigned to the linear $Q^2(0,2)$ as reported by Marsmann et al.[14] and the others at −91.40 and −92.40 ppm have been attributed to cyclic $Q^2(1,1)$ and linear $Q^2(1,1)$ species, respectively. That is quite in agreement with the values of −91.30 and −92.30 ppm, respectively, proposed by Marsmann et al.[14] At this stage no Q^3 or Q^4 species are visible (Figure 3) so that only cyclic trimer or tetramer species can be expected in this experiment (w = 2.8).

B. Excess H_2O. With excess water (w = 8) the polarization transfer becomes inefficient because most OCH_3 groups are exchanged with OH groups, and the hydroxyl protons do not contribute to signal enhancement because they are exchanged too rapidly. Standard single-pulse acquisition is not practical either

(14) Marsmann, H. C.; Meyer, E.; Vongehr, M.; Weber, E. F. *Makromol. Chem.* **1983**, *184*, 1817.

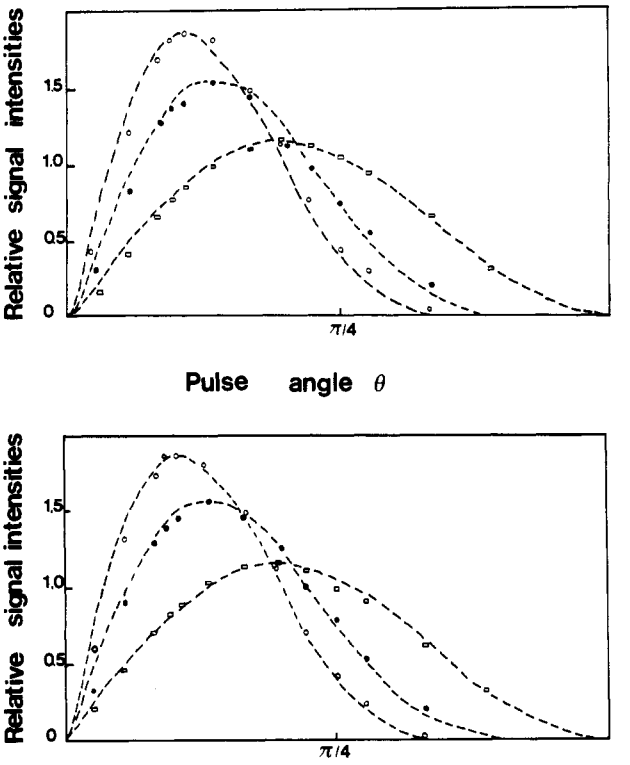

Figure 4. (a, top) Experimental relative signal intensities (points) and theoretical curves (dotted lines) for DEPT with variable pulse angle for resonances belonging to the monomeric group Q^0: (-○-) $Q^0(1,3)$:Si-$(OCH_3)_3OH$, δ = −76.15 ppm; (-●-) $Q^0(2,2)$:$Si(OCH_3)_2(OH)_2$, δ = −74.60 ppm; (-□-) $Q^0(3,1)$:$Si(OCH_3)(OH)_3$, δ = −73.45 ppm. Chemical shifts are given in ppm relative to TMS with positive shifts downfield. (b, bottom) Experimental relative signal intensities (points) and theoretical curves for DEPT with variable pulse angle θ for resonances belonging to the Q^1 group: (-○-) $Q^1(0,3)$:Si-O-Si$)OCH_3)_3$, δ = −85.85 ppm; (-●-) $Q^1(1,2)$:Si-O-$Si(OCH_3)_2OH$, δ = −84.15 ppm; (-□-) Q^1-(2,1):Si-O-$Si(OCH_3)(OH)_2$, δ = −82.80 ppm.

TABLE I: Chemical Shifts of Q^0, Q^1, Q^2, Q^3, and Q^4 in the Mixtures (A) $TMOS/CH_3OH/H_2O$ = 1/3.7/2.8 (pH = 3.0) and (B) $TMOS/CH_3OH/H_2O$ = 1/3.7/8 (pH = 3.0)

A	B	species
−78.25		$Q^0(0,4)$:$Si(OCH_3)_4$
−76.15		$Q^0(1,3)$:$Si(OCH_3)_3(OH)$
−74.60	−74.70	$Q^0(2,2)$:$Si(OCH_3)_2(OH)_2$
−73.45	−73.60	$Q^0(3,1)$:$Si(OCH_3)(OH)_3$
−72.40	−72.70	$Q^0(4,0)$:$Si(OH)_4$
−85.85	−84.40	$Q^1(0,3)$:$Si(OCH_3)_3OSi$-
−84.15	−83.60	$Q^1(1,2)$:$Si(OCH_3)_2(OH)OSi$
−82.80	−83.05	$Q^1(2,1)$:$Si(OCH_3)(OH)_2OSi$
−81.80	−82.10	$Q^1(3,0)$:$Si(OH)_3OSi$
	−90.15	
	−90.90	cyclic $Q^2(2,0)$
−91.40	−91.65	cyclic $Q^2(1,1)$
−92.40	−92.75	linear $Q^2(1,1)$
−93.70		linear $Q^2(0,2)$
	−98.60 (pH = 1.5)	$Q^3(1,0)$
	−99.50 (pH = 1.5 and 2.0)	$Q^3(1,0)$
	−100.65 (all pH)	
	−101.75 (pH = 2.6 and 3.0)	
	−110	Q^4

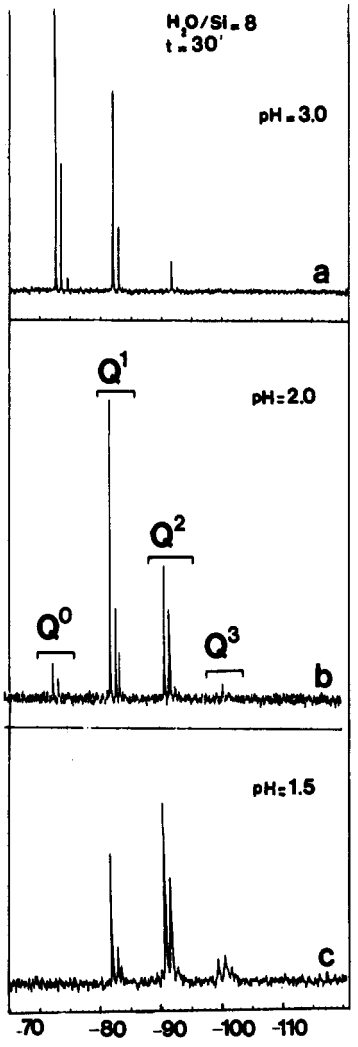

Figure 5. ^{29}Si NMR spectra of the $TMOS/CH_3OH/H_2O$ mixture in 1/3.7/8 molar ratio obtained at 295 K after 30 min using the spin-echo method with inverse-gated decoupling (decay time 30 ms and number of transients 56): (a) pH = 3.0; (b) pH = 2.0; (c) pH = 1.5.

because the broad ^{29}Si resonance around 110 ppm from the glass tube and probe insert overlaps the lines of the more condensed species Q^3 and Q^4. Then the best way to record spectra is the spin echo sequence (90°–τ_{ref}–180°–observation of a free induction echo at $2\tau_{ref}$) because ^{29}Si in the solid glass have a much shorter T_2 than those in the gel and do not contribute to the echo if τ_{ref} exceeds their T_2. The refocusing time τ_{ref} was determined to be 30 ms.

With excess water (w = 8) more condensed species Q^2, Q^3, and Q^4 appear at early steps of the polymerization (Figure 5) and after 10 h their proportion increased greatly (Figure 6). Figure 7 shows the multiplets that are observed through this method at long times; the Q^2 units give a group of two intense multiplets and the major peaks are reported in Table I. The major resonance at −90.90 ppm (b) that becomes more intense at decreasing pH is probably due to a Q^2 unit with two OH groups. This seems in good agreement with Wies et al.[15] who proposed a tetracyclic $Q^2(2,0)$ for the signal at −90.90 ppm and with the value of −90.60 ppm recently reported by Pouxviel et al.[3] for cyclic $Q^2(2,0)$. The $Q^2(2,0)$ unit has been also proposed by Marsmann et al.[14] for the resonance at −90.50 ppm. The minor peaks (a, c, and d) have not been attributed. The two multiplets near −91.65 ppm (e and f) could be assigned to cyclic $Q^2(1,1)$ species but the two remaining

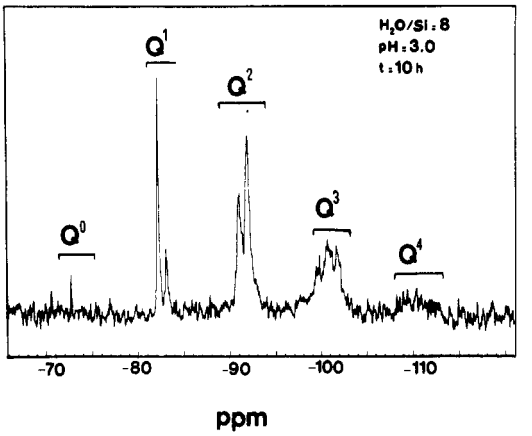

Figure 6. ^{29}Si NMR spectra of the $TMOS/CH_3OH/H_2O$ mixture in 1/3.7/8 molar ratio at 295 K and pH = 3.0 after 10 h.

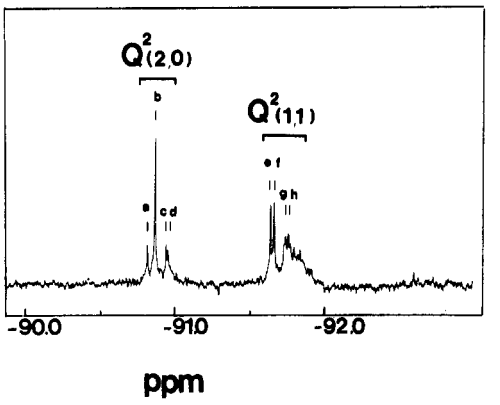

Figure 7. Expanded spectra of the $TMOS/CH_3OH/H_2O$ mixture in 1/3.7/8 molar ratio at 295 K and pH = 3.0 after 10 h (Q^2 resonance): (a) −90.80 ppm; (b) −90.90 ppm; (c) −90.95 ppm; (d) −90.98 ppm; (e) −91.63 ppm; (f) −91.67 ppm; (g) −91.74 ppm; (h) −91.77 ppm.

peaks (g and h) in the Q^2 region cannot be attributed without further data. The resonance at −93.70 ppm previously attributed to a Q^2 unit with two −OR groups[14] is no longer observed in agreement with a higher water to SiOR ratio.

The Q^3 units appear generally in the shift range of about −99 to −103 ppm and are less well resolved than Q^2 units, particularly at long times when condensation reactions increase (Figure 6) and are characteristic of highly polymerized species. Resonances at lower field (−98.60 and −99.50 ppm) could arise from hydrolyzed species $Q^3(1,0)$. But precise data on assignments on the chemical shifts in this complex region are lacking and other investigations are in progress. At pH = 3.0 a large ($\Delta\nu$ = 150 Hz) unresolved signal is visible about −110 ppm caused by the resonance of Q^4 units[8] but no specific species can be identified.

Results and Discussion

Now the quantitative distribution of ^{29}Si among the various species can be obtained from the relative intensities of the corresponding lines.

A. Stoichiometric Concentrations of H_2O. During the first 2 h the TMOS is quickly replaced by hydrolyzed monomers $Si(OCH_3)_{4-n}(OH)_n$ (n = 1, 2, 3, and 4) (Figure 8a). The n = 1 monomer is formed much faster than the others and its concentration decays as that of TMOS. For the others the concentration reaches a maximum after 2 h. This maximum concentration is smaller for the more highly hydrolyzed ones and hence the hydrolysis depends upon the degree of substitution of the monomers.[3,16] Here the important point is that the concentration of the fully hydrolyzed monomer (n = 4) remains below 10% and hence the hydrolysis is very incomplete at this stage.

(15) Wies, Ch.; Meise-Gresch, K.; Müller,-Warmuth, W.; Beier, W.; Göktas, A. A.; Frischat, G. H. *Ber. Bunsen-Ges. Phys. Chem.* **1988**, *92*, 689.

(16) Turner, C. W.; Franklin, K. J. *J. Non-Cryst. Solids* **1987**, *91*, 402.

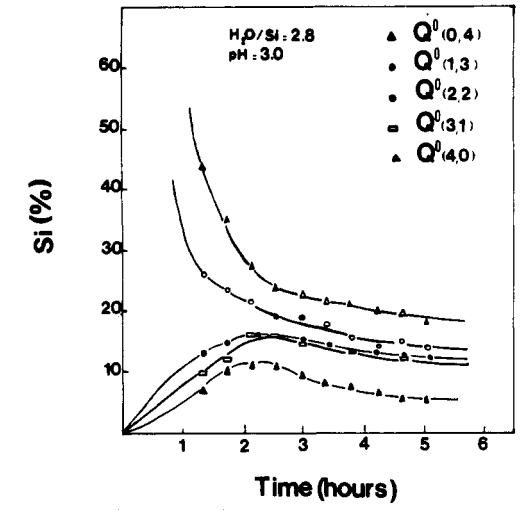

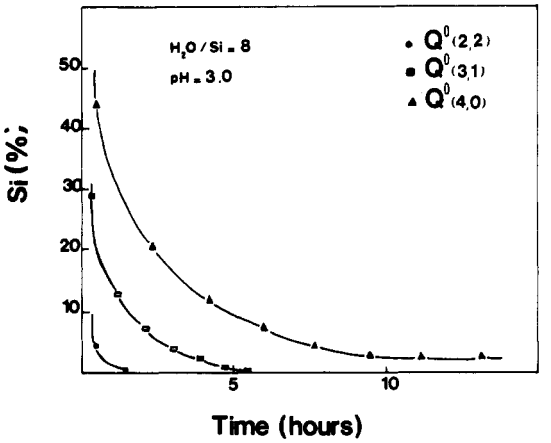

Figure 8. (a, top) Time evolution of relative concentrations of species Q^0 in the $TMOS/CH_3OH/H_2O$ mixture in 1/3.7/2.8 molar ratio at pH = 3.0. (b, bottom) Time evolution of relative concentrations of species Q^0 in the $TMOS/CH_3OH/H_2O$ mixture in 1/3.7/8 molar ratio at pH = 3.0.

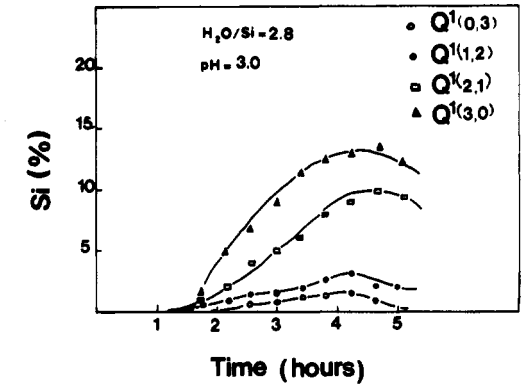

Figure 9. Time evolution of relative concentrations of condensed species Q^1 in the $TMOS/CH_3OH/H_2O$ mixture in 1/3.7/2.8 molar ratio at pH = 3.0.

After 2 h condensation reactions begin and the maximum concentration of dimers or chain ends Q^1 is reached after 4 h (Figure 9). The proportion of Q^1 species with two or three alkoxide groups $Q^1(1,2)$, $Q^1(0,3)$ is negligible (below 5%) while the concentration of $Q^1(3,0)$ is higher (15%). Hence the chain ends are largely hydrolyzed at this stage, and further condensation will occur mostly between hydrolyzed groups according to eq 2b. Indeed, it is known that silanols are unstable intermediates[17] and that the dimerization rate between the monomers $Si(OCH_3)_{4-n}$-

(17) Brinker, C. J.; Keefer, K. D.; Wschaeffer, D.; Assink, R. A.; Kay, B. D.; Ashley, C. S. *J. Non-Cryst. Solids* **1984**, *63*, 45.

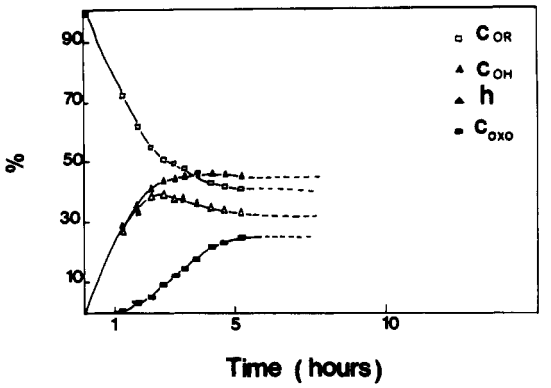

Figure 10. Time evolution of parameters c_{OR}, c_{OH}, h (hydrolysis ratio), and c_{oxo} (condensation ratio) in the $TMOS/CH_3OH/H_2O$ in 1/3.7/2.8 molar ratio at pH = 3.0.

$(OH)_n$ becomes higher as n increases from 1 to 4.[18] The other reaction path (eq 2a) does not become important unless the ratio of water to alkoxide is much lower than the stoichiometry.[19]

It is instructive to follow the reactions according to the proportions of –OR and –OH remaining groups, as defined by Pouxviel et al.[3]:

$$c_{OR} = \{Si\text{–}OR\}/4\{Si\}$$

$$c_{OH} = \{Si\text{–}OH\}/4\{Si\}$$

The hydrolysis ratio (h) and the condensation ratio (c_{oxo}) are defined as

$$h = (\{Si\text{–}OH\} + \{\text{–}O\text{–}\})/4\{Si\}$$

$$c_{oxo} = 2\{\text{–}O\text{–}\}/4\{Si\}$$

where {–O–} is the number of bridging oxygens and {Si} the total number of Si atoms. The following relation can be deduced:

$$c_{OR} + c_{OH} + c_{oxo} = 1$$

The time evolution of these parameters for the system H_2O/TMOS = 2.8 and pH = 3 is presented in Figure 10; c_{OR} decays rapidly in the first 2 h and then stabilizes about 40% and hence the hydrolysis is not complete. Similarly, c_{OH} saturates around 40% after 2 h. The hydrolysis ratio (h) increases as c_{OH} during 1.5 h and then reaches a maximum value at h = 45%. The condensation ratio (c_{oxo}) begins to increase after only 1 h to reach the maximum value of 25% after 5 h. This incomplete hydrolysis is similar to that observed by Pouxviel et al.[3] for $H_2O/TEOS$ = 4 and pH = 2.5. After 2.5 h the calculated values by Pouxviel et al.[3] of c_{OR} (25%) and c_{OH} (65%) are in good agreement with our results.

Next, a global equation that corresponds to the average of the different hydrolysis reactions can be written and a "pseudo rate constant" k_h can be defined, taking into account only the nature[18] of the functional groups OR and OH as proposed by Orcel et al.[20]

$$\text{–Si–OR} + H_2O \xrightarrow{k_H} \text{–Si–OH} + ROH \qquad (4)$$

with $-d/dt\ \{Si\text{–}OR\} = k_h\{SiOR\}\{H_2O\}$.

In the same way, a pseudo rate constant k_c can be defined from the global condensation reaction

$$\text{–Si–OH} + \text{HO–Si–} \xrightarrow{k_c} \text{–Si–O–Si–} + H_2O \qquad (2b)$$

with $d/dt\ \{Si\text{–}O\text{–}Si\} = k_c\{Si\text{–}OH\}^2$.

The values of k_h and k_c can be estimated from the evolution of the parameters c_{OR}, c_{OH}, h, and c_{oxo} (Figure 10). During the early stage where condensation has not yet begun ($t < 2$ h), the concentrations of Si–OR and H_2O will remain roughly propor-

(18) These global rate constants are not true rate constants because the reactivity of the functional groups –OR and –OH is dependent of the degree of substitution or polymerization of the Si.

(19) Assink, R. A.; Kay, B. D. In *Better Ceramics Trough Chemistry*; Brinker, C. J., Clark, D. E., Ulrich, D. R., Ed.; Material Research Society: New York, 1985; p 32.

(20) Orcel, G.; Hench, L. *J. Non-Cryst. Solids* **1986**, *79*, 177.

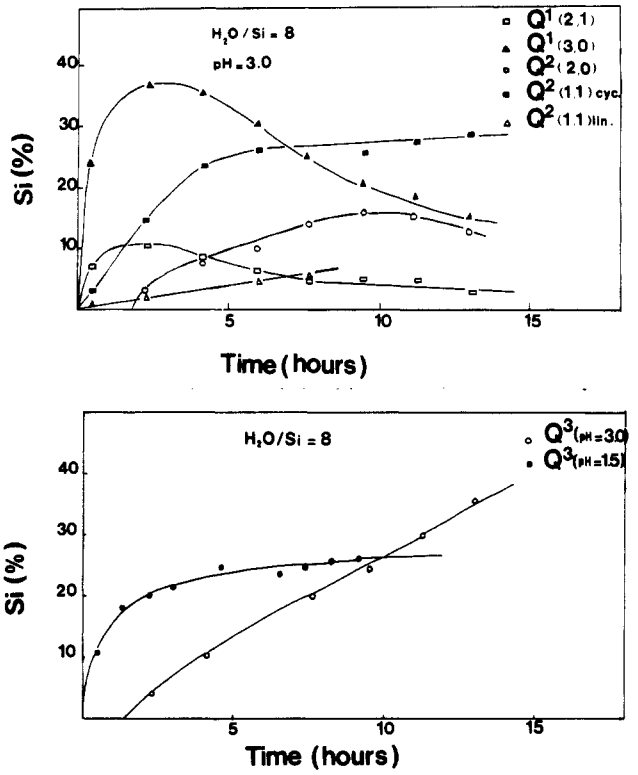

Figure 11. (a, top) Time evolution of relative concentrations of species Q^1 and Q^2 in the $TMOS/CH_3OH/H_2O$ mixture in 1/3.7/8 molar ratio at pH = 3.0. (b, bottom) Time evolution of relative concentrations of species Q^3 in the $TMOS/CH_3OH/H_2O$ mixture in 1/3.7/8 molar ratio at pH = 3.0 and pH = 1.5.

tional to each other because the initial composition of the mixture is nearly stoichiometric:

$$\{H_2O\}_t = 0.7\{Si\text{–}OR\}_t$$

This results in a second-order kinetics:

$$-d/dt\ \{Si\text{–}OR\} = k_h\{Si\text{–}OR\}\{H_2O\}$$

$$= 0.7k_h\{Si\text{–}OR\}^2$$

Integration yields

$$1/\{Si\text{–}OR\} = 1/\{Si\text{–}OR\}_0 + 0.7k_ht$$

From the plot of $1/\{Si\text{–}OR\}$ versus time the value of the hydrolysis rate constant k_h can be obtained: $k_h = 4.6 \times 10^{-2}$ L mol^{-1} h^{-1} (second-order kinetics). This value is in fairly good agreement with the values found by Pouxviel et al.,[3] $k_h = 14 \times 10^{-2}$ L mol^{-1} h^{-1} for $H_2O/TEOS = 4$ and pH = 2.5, and by Orcel et al.,[20] $k_h = 1.2 \times 10^{-2}$ L mol^{-1} h^{-1} at pH = 5.5 because k_h increases with H^+.

During the second stage where c is nearly constant, hydrolysis reactions can be neglected and from eq 2b it may be written

$$-d/dt\ \{Si\text{–}OH\} = d/dt\ \{Si\text{–}O\text{–}Si\} = k_c\{Si\text{–}OH\}^2$$

Integration yields $1/\{Si\text{–}OH\} = k_ct$.

From the experimental values of c_{OH} (Figure 11) the condensation rate can be estimated as $k_c = 1.8 \times 10^{-2}$ L mol^{-1} h^{-1}, in agreement with the value[3] $1.4 \times 10^{-2} < k_c < 6.4 \times 10^{-2}$ L mol^{-1} h^{-1}. At this stage we conclude that $k_c < k_h$ in the pH range 1–3 and hence the condensation is rate limiting.[21-23]

B. Concentrations of H_2O in Excess. In this section we present the results obtained with H_2O in excess ($H_2O/TMOS = 8$) and variable concentrations of HCl (pH values from 3.0 to 1.5). The ^{29}Si NMR spectrum obtained after 30 min in the mixture

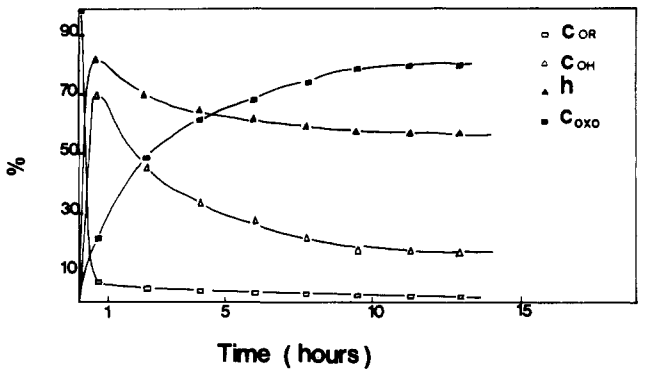

Figure 12. Time evolution of parameters c_{OR}, c_{OH}, h (hydrolysis ratio), and c_{oxo} (condensation ratio) in the $TMOS/CH_3OH/H_2O$ mixture in 1/3.7/8 molar ratio at pH = 3.0.

$TMOS/CH_3OH/H_2O$ = 1/3.7/8 and pH = 3.0 is shown in Figure 5a. Comparison between Figure 3a and Figure 5a clearly indicates that the hydrolysis is faster and more complete. The initial precursor $Q^0(0,4)$ has completely disappeared and only the resonances corresponding to well-hydrolyzed monomers $Si(OH)_4$ and $Si(OR)(OH)_3$ are intense. After 30 min the proportion of $Si(OH)_4$ represents 50% instead of 10% (Figure 8b) with stoichiometric amount of water. The concentration of dimers Q^1 is also more important (40% for $Q^1(3,0)$ instead of 15%) and the maximum value is obtained after only 2 h (Figure 11a). After 10 h the concentration of condensed species is about 15% for Q^1 units, 40% for Q^2, 35% for Q^3, and 5% for Q^4 (Figure 11, a and b). In particular it appears that the proportion of Q^3 chain branching sites has greatly increased and that highly branched polymeric species are present.

Again these reactions can be followed according to the values of the global parameters c_{OR}, c_{OH}, h, and c_{oxo}. The comparison of Figure 12 and Figure 10 shows indeed that hydrolysis is faster and more complete and consequently condensation starts earlier and it keeps increasing up to a saturation value (c_{oxo} = 80% after 10 h). This last value is quite high and indicates that the polymers are made of highly condensed subunits.

Pseudo rate constants can be defined as above. Hydrolysis is still described by the equation

$$-d/dt\ \{Si\text{–}OR\} = k_h\{Si\text{–}OR\}\{H_2O\}_0$$

but now the H_2O concentration is nearly constant and the integration yields

$$\{Si\text{–}OR\} = \{Si\text{–}OR\}_0e^{-k_h(H_2O)_0t}$$

The hydrolysis rate obeys first-order kinetics and a plot of log $\{Si\text{–}OR\}/\{Si\text{–}OR\}_0$ versus time yields $k_h = 25 \times 10^{-2}$ h^{-1}. This value is very close to that found by Pouxviel et al.:[3] $k_h = 23 \times 10^{-2}$ h^{-1} for $H_2O/TEOS = 10$ and pH = 2.5.

A comparison of the rate constants obtained at different pH values indicates clearly that the hydrolysis rate constant increases with H^+ concentration (Figure 15) according to the dependence[24]

$$\log k_h = \log H^+ + b$$

where b is solvent dependent. Our results are in good agreement with the electrophilic mechanism proposed by Aelion et al.[24]

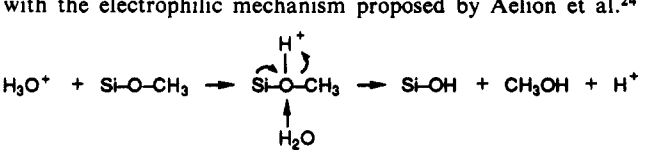

The proton attracted by the negative charge of oxygen in the OCH_3 group leads to a charge transfer from silicon toward oxygen. So the positive charge of silicon increases and the alkoxide group is eliminated and replaced by hydroxide group (harder π donor).

The effect of pH on the condensation rate is dependent on the stages of the reaction; at short times and at lower pH value (1.5)

(21) Brinker, C. J.; Keefer, K. D.; Schaefer, D. W.; Ashley, C. S. *J. Non-Cryst. Solids* **1982**, *48*, 47.
(22) Assink, R. A.; Kay, B. D. *Mater. Res. Soc. Symp. Proc.* **1984**, *32*, 301.
(23) Schaefer, D. W. *Rev. Phys. Appl.* **1989**, *24*, C4-121.
(24) Aelion, R.; Loebel, A. *J. Am. Chem. Soc.* **1950**, *72*, 5705.

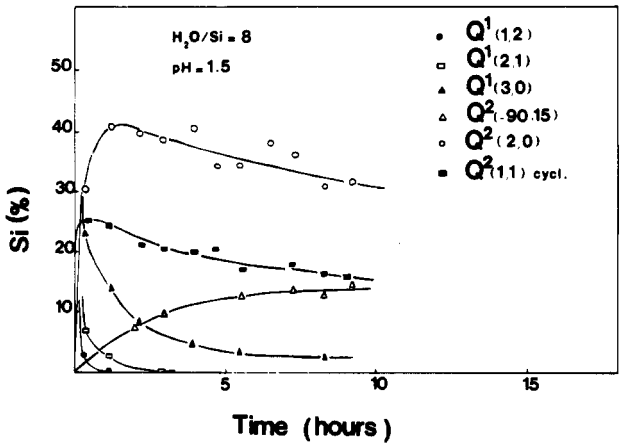

Figure 13. Time evolution of relative concentrations of species Q^1 and Q^2 in the $TMOS/CH_3OH/H_2O$ mixture in 1/3.7/8 molar ratio at pH = 1.5.

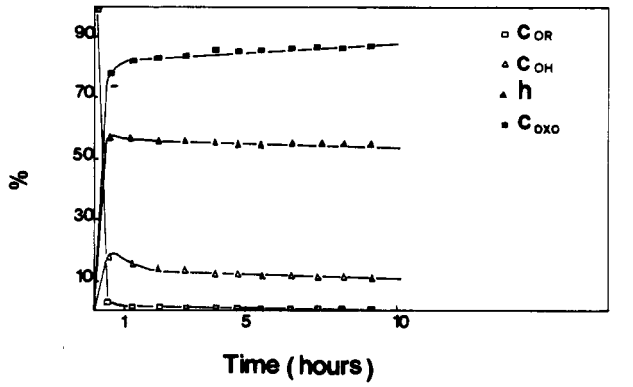

Figure 14. Time evolution of parameters c_{OR}, c_{OH}, h (hydrolysis ratio), and c_{oxo} (condensation ratio) in the $TMOS/CH_3OH/H_2O$ mixture in 1/3.7/8 molar ratio at pH = 1.5.

the linear and cyclic species Q^2 rise sooner, at the expense of dimers or chain ends Q^1 (Figure 13). The more condensed species Q^3 also start sooner (Figure 11b) but they grow more slowly: after 13 h the proportion of branching sites $Q^3(1,0)$ is only 25% compared with 35% for the reaction at pH = 3.0 (Figure 11b). Hence condensation starts sooner at lower pH because the hydrolysis is completed earlier, but it proceeds slowly in agreement with the nucleophilic mechanism proposed by Iler[2] for the condensation reaction:

$$Si\text{–}O^- + HOSi \rightarrow HO^- + Si\text{–}O\text{–}Si \qquad (5)$$

The evolution of the global parameters c_{OR}, c_{OH}, h, and c_{oxo} shows that the early stages of the reaction (Q^0–Q^1–Q^2) are all completed in an hour (Figure 14). Of course the later stages do not show up on this graph, since they involve mainly the transformation of Q^2 into Q^3 which does not affect the values of these parameters. At long reaction times ($t > 10$ h) (Figures 12 and 14) the condensation rate constants can be estimated: at pH = 3.0 a k_c value of 6.2×10^{-2} L mol^{-1} h^{-1} is obtained whereas at pH = 1.5 k_c is approximately 0.10 L mol^{-1} h^{-1}. These values are in agreement with that found by Pouxviel et al.[3] for H_2O/TEOS = 10 and pH = 2.5: $k_c = 1.7 \times 10^{-2}$ L mol^{-1} h^{-1} after 10 h. Figure 16 displays the observed time dependence of the Q^i species for $w = 8$ and pH = 3. The necessary time to reach the maximum concentration of the Q^i species increases as i increases from 1 to 4. It arises from the successive stages of the condensation reaction: Q^0–Q^1 Q^2.... A distribution of this type with different formation rates for the Q^i species has been observed by Assink et al.[22] They present a statistical reaction model in order to take into account the distribution of the various functional groups (–OR, –OH, and –OSi) about the silicon atoms. Comparison with our experimental results seems to indicate a good agreement with statistically equilibrium distributions. Nevertheless a more complete kinetic model would require distinction between the numerous distinct local silicon chemical environments.

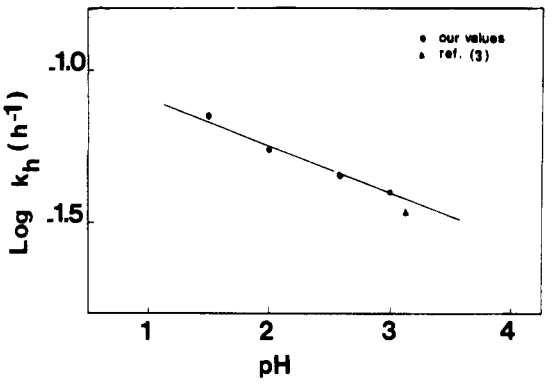

Figure 15. Variation of the hydrolysis rate constant k_h with the acid concentration in the $TMOS/CH_3OH/H_2O$ mixture in 1/3.7/8 molar ratio.

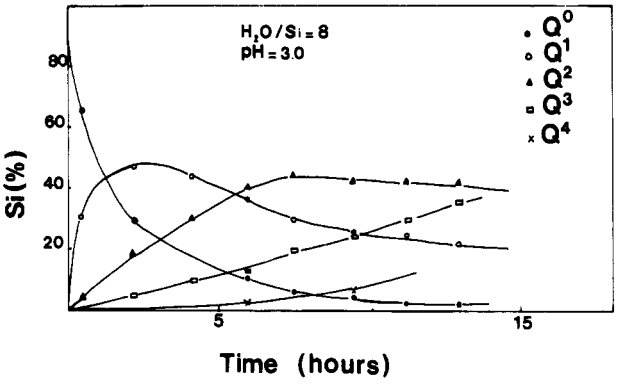

Figure 16. Time evolution of relative concentrations of species Q^0, Q^1, Q^2, Q^3, and Q^4 in the $TMOS/CH_3OH/H_2O$ mixture in 1/3.7/8 molar ratio at pH = 3.

Conclusion

High-resolution ^{29}Si NMR spectroscopy has been employed to follow the hydrolysis–condensation reaction of the mixture $TMOS/CH_3OH/H_2O$ in acidic conditions. By use of polarization-transfer experiments various hydrolyzed monomeric and low-order polymeric species (Q^1, Q^2, and some Q^3 units) have been identified. From the intensities of resonances, the quantitative distribution of species has been obtained, and rate parameters (k_H, k_C, ...) have been calculated.

It is found that the hydrolysis and condensation of TMOS are largely determined by the amount of water available for hydrolysis and by the concentration of H^+ ions that catalyze this reaction.

At substoichiometric ratios of water to TMOS ($w = H_2O$/TMOS = 2.8) the hydrolysis is incomplete (only 40% for hydrolysis ratio). Consequently the condensation is slow to start and very incomplete (only 25% condensation after 5 h).

With an excess of water ($w = 8$) hydrolysis is fast and complete, condensation starts sooner and it is much more extensive; the overall condensation ratio is beyond 80%, with 15% end groups of chains (Q^1), 40% middle chain or ring groups (Q^2), and 35% chain branching sites (Q^3). Thus the polymers are highly branched or made of subunits including ring or cage structures, which is the same on a local scale.

The effect of H^+ on the early stages of the reaction is to increase the rate of hydrolysis. Even at comparatively long reaction times, a sizeable fraction of species are not fully hydrolyzed (compare Figure 11 with Figure 13). The other main conclusion concerns the effect of H^+ on the condensation reactions, which is shown in Figure 11b. Large H^+ concentrations favor the growth of polymers that have more linear sections. Low H^+ concentrations favor the growth of polymers that are more extensively branched. If predominantly linear polymers are desired, it will be necessary to use low ratios of water to monomer and high H^+ concentrations.

Registry No. Silicon tetramethoxide, 681-84-5.